Water, Energy, Food and Environment Journal
An International Journal

http://dx.doi.org/10.18576/wefej/010103

Performance Analysis, Mathematical Modeling and Economic Assessment of Developed Vacuum Membrane Distillation System for Water Desalination

Elham El-Zanati[*] *and Maaly Khedr.*

Chemical Engineering and Pilot Plant Department, Engineering Research Division, National Research Centre, 33El-Bohouth St. (Former El Tahrir St.), Dokki, Giza, Egypt.

Received: 25 Mar. 2019, Revised: 22 Apr. 2019, Accepted: 5 Aug. 2019.
Published online: 1 Jan. 2020.

Abstract: Membrane distillation is a thermal and pressure driven process through hydrophobic microporous membranes, it is a promising technology for water desalination. In this work, an experimental study of vacuum membrane distillation (VMD), was implemented on lab and pilot scales, using an early prepared hydrophobic microporous membrane (polyethersulfone/tetraethoxysilane). The system performance is assessed, using an aqueous NaCl solution, at different concentrations (25,000 - 40,000 ppm), different temperatures (298-338 K), different flow rates (0.000008 to 0.000028 m^3s^{-1}) and different permeate vacuum pressure (200-800 mbar). The obtained results proved that the designed and installed system reached a salt rejection of 99% with a membrane flux of 25 kg/m^2hr at 338 K and 300 mbar gauge. Moreover, a mathematical model was developed to describe the VMD. The model was verified using the obtained experimental results. Furthermore, cost indicators were estimated based on a local offer for manufacturing a VMD unit of 2.6 m^3d^{-1} capacity. Expected that, in comparison to RO, when MD is fully developed at a large scale and using low-grade energy source, it should be lower in capital cost and operating expenses.

Keywords: desalination; vacuum membrane distillation; hydrophobic porous membrane; modeling, pilot investigation.

1 Introduction

Regarding the growth of the world population, several developing countries suffer from water scarcity. The limited resources and the progressively increased requirements for fresh water are a crucial problem [1]. Hence, to surmount this problem, effective water programs in many regions of the world would be practiced. Water desalination is an excellent alternative. The technologies used on the industrial scale are generally categorized into two categories: thermal processes (Multi-Stage Flash distillation, Multi-Effect Distillation, Vapor Compression) and membrane processes (Reverse Osmosis and Electro Dialysis Reversal). While those technologies are commercialized, they are energy consuming, have scale problems, and related operational problems. Alternative recent technology; Membrane Distillation (MD) is considered the future technology due to its prospective merits regarding energy consumption, simplicity and its ability to be coupled with solar energy [2,3]. MD a new process employed in desalination and water treatment. Based on the temperature and pressure differences, the water evaporates through the hydrophobic microporous membrane, that ensures high water purity irrespective of feed quality, and the water vapor condenses into a freshwater stream [1,4,5]. The driving force for mass transfer in MD is the vapor pressure difference induced by a temperature gradient across the membrane. Because the partial vapor pressure of water is only minimally affected by increased concentrations of dissolved salts, MD has the potential to be an ideal method for high saline feeds.

Correspondingauthore-mail: eelzanati@gmail.com

The merits of MD are: a complete rejection of salts, macromolecules, and non-volatile compounds; lower operating temperatures than conventional distillation; significant lower hydrostatic operating pressures than conventional pressure-driven membrane separation processes; in this respect, a less expensive material involves; MD has the ability to utilize renewable energy sources [7,8,9]; MD can potentially minimize brine volume at lower energy expenditure and with less complexity [5]; reduced vapor spaces compared to conventional distillation processes [5].

Depending on the method used to induce the vapor pressure gradient across the membrane, the MD classified into four configurations: *i- Direct Contact Membrane Distillation (DCMD), ii- Air Gap Membrane Distillation (AGMD), iii- Sweep Gas Membrane Distillation (SGMD), iv- Vacuum Membrane Distillation (VMD).*

The microporous hydrophobic membranes regularly made of PTFE, PVDF, also, a physically or chemically modified PES [4].

In VMD, the cold-water stream flows under negative pressure (vacuum). Under specific operating conditions [5]. The permeate flux is dependent on vapor pressure differences.

In this study, the aim is to investigate experimentally the performance of a novel hydrophobic polyethersulphone-based porous membrane for water desalination (previously prepared and characterized [10]); to develop and verify a mathematical model that is talented to describe the essential phenomena in VMD; and finally, to design, implement and economically appraise a pilot VMD system.

2 Experimental

2.1 Lab-Scale Experimental Set-Up

The experimental analysis of Vacuum Membrane Distillation (VMD) was performed on a lab-scale unit, as illustrated in Figure (1) [8], using flat membrane holder imported from Zulassige (Germany manufacturer), it contains three openings; to applying vacuum pressure, to feeding and to recycling the concentrate to the feeding tank.

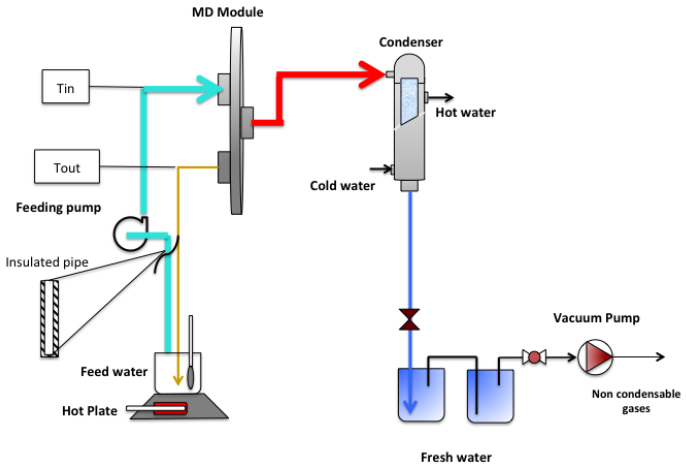

Fig.1: Schematic diagram of VMD experimental laboratory setup.

The feed was continuously fed to the membrane module from a glass feeding vessel using a peristaltic pump. Vacuum pressure was developed using a vacuum pump. The system is equipped with a measurement and control system. The feed and permeate streams are insulated. The difference in temperature and pressure between the feed and permeate sides makes water to vaporize through membrane pores, the vapor was drawn and condensed using a chiller at 5°C temperature.

These experiments were performed using the earlier prepared and tested hydrophobic porous membrane Polyethersulfone/Tetraethylorthosilicate, PES/TEOS [10], the porosity and thickness are 0.7 and 153 µm respectively. They are carried out at different operating conditions, to study the effect of various process parameters like vacuum pressure, feed water concentration, etc.

2.2 Design and Implementation of a Pilot Vacuum Membrane Distillation Unit

A pilot membrane distillation (VMD) unit was designed and manufactured in a local factory. The formerly prepared hydrophobic porous membrane, (PES/TEOS), was used to study the performance of the unit. The design basis, summarized in Table (1), was relying on the results achieved experimentally.

Table 1: Design basis of Vacuum Membrane Distillation pilot unit.

Parameter	**Value**
Permeate flux, L/m^{2}h	20-30
Membrane Salt rejection %	97-99
Unit capacity, m^3/d	1.2
Feed temperature, K, (^{o}C)	338, (65)
Absolute pressure, kPa	0.03

Figure (2) illustrates the process flow diagram of the integrated system of VMD. It consists of a feeding plastic tank of volume 3 m^3. A Stainless-Steel centrifugal pump uses to feed the unit, by a synthetic salt solution, the discharge flow rate ranges from (0.000008 to 0.000028 m^{3}s^{-1}). The Stainless-Steel module consists of two correctly closed square discs of 50 cm width, one of them has two openings (feed water/effluent of the concentrate), while, the second disc has one opening to escape the vapor, which is directed to a Stainless-Steel condenser to recover the permeate. The effective area of the membrane is 0.2 m^2. The module has a Teflon screen mesh to support the membrane.

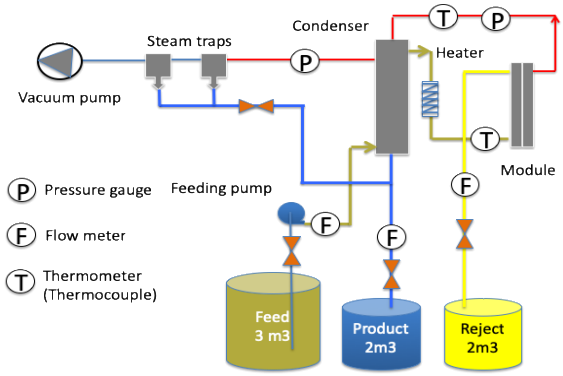

Fig. 2: Schematic diagram for pilot test vacuum membrane distillation.

A condenser of two concentric tubes and a heat transfer area of 0.01 m^2, is connected to the outlet of the membrane module.

Condensation is carried out using a circulating chiller. A high vacuum pump (Acculab double stage, 2VP-3C) is connected to the condenser to create the vacuum in the system. All hot parts and connections of the unit are well isolated. The system is associated with an electrical panel and well equipped with instrumentation tools for conductivity, temperature, pressure and flow rate monitoring.

3 Development of Mathematical Model for Vacuum Membrane Distillation

3.1 Mass Transfer Model

In vacuum membrane distillation, simultaneous heat and mass transfer process occur, resulting in heat and mass fluxes across the hydrophobic membrane. Figure (3) demonstrates a membrane element considering the feed and permeate conditions and corresponding equilibrium concentration, pressure, and temperature.

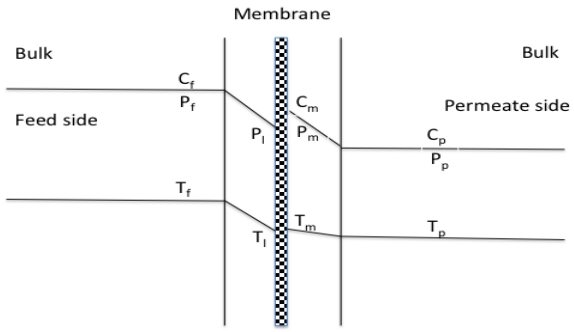

Fig.3: Membrane element of Vacuum Membrane Distillation.

The mass transfer occurs by convective and diffusive transport of water vapor across the hydrophobic microporous membrane. The driving force for mass transfer is the difference of water vapor pressure between both sides of the membrane. Resistance to mass transfer comes from both; the membrane structure, and the presence of air trapped within the membrane. By neglecting the effect of air, the diffusion is described either by the Knudsen diffusion or the Poiseuille flow models. The former is being dominant in case the pore size is smaller than the mean free path of the water vapor molecules, while the latter is governing when the membrane pore size is larger than the mean free molecular path. Expected, that the membrane pores are particularly small than the mean free path of the diffusing water vapor molecules, besides, the vacuum on the permeate side of the membrane avoids the formation of a boundary layer, therefore, the resistance can be ignored [11,12,13]. The mass flux of the Knudsen diffusion model is expressed as:

$$N_{Kn} = 1.064 \frac{r\varepsilon}{\tau\delta}\left(\frac{M}{RT_m}\right)^{0.5}(P_1 - P_o) \quad (1)$$

$$N_P = 0.125 \frac{r^2\varepsilon}{\tau\delta}\frac{MP_m}{\eta RT_m}(P_1 - P_o) \quad (2)$$

Figure (4) demonstrates the schematic flow diagram of the VMD system, the temperature difference at the two sides of the membrane creates a vapor pressure gradient inside membrane pores, which causes a mass flux through the membrane.

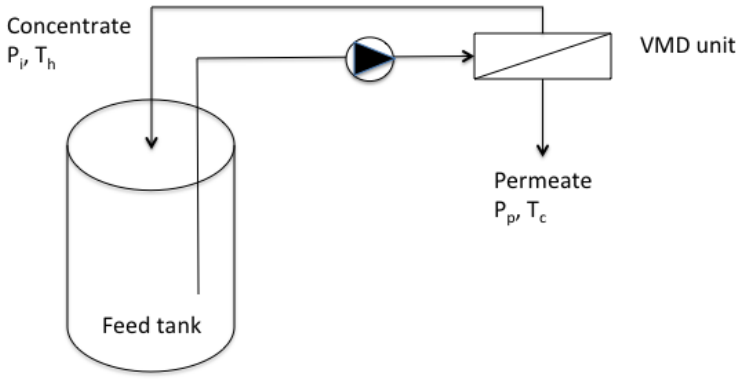

Fig.4: Schematic drawing of the VMD process.

3.2 Model Derivation

By considering negligible mass transfer resistance caused by molecule-molecule collision, by developing mass balance on feed tank and by suggesting diffusion process within the pores, controlled by Knudsen diffusion and Poiseuille diffusion, equation (3) expresses the mass flux:

$$\frac{dN}{dt} = -N_{Kn}A_m - J_s A_m \quad (3)$$

$$\frac{dN}{dt} = -1.064\,\frac{r\varepsilon}{\tau\delta}\left(\frac{M}{RT_m}\right)^{.5}(P_1 - P_o)A_m - 0.125\,\frac{r^2\varepsilon}{\tau\delta}\frac{MP_m}{\mathfrak{y}RT_m}(P_1 - P_o)A_m - K_s\,(c_o - c)A_m \quad (4)$$

Where:

$$J_s = K_s\,(c_o - c) \quad (5)$$

$$\frac{dV}{dt} = -\frac{A_m}{\rho}\left\{\left[-1.064\,\frac{r\varepsilon}{\tau\delta}\left(\frac{M}{RT_m}\right)^{.5} - .125\,\frac{r^2\varepsilon}{\tau\delta}\frac{MP_m}{\mathfrak{y}RT_m}\right](P_1 - P_o) - K_s\,(c_o - c)\right\} \quad (6)$$

$$(P_1 - P_o) = \frac{dP}{dT}(T_1 - T_o) \quad (7)$$

$$\frac{dP}{dT} = \frac{P\lambda M}{RT_m^2} \quad \text{at } T_m \quad (8)$$

$$P = exp\left(23.238 - \frac{3841}{T_m - 45}\right) \quad (9)$$

$$(T_1 - T_o) = \tau_m\,(T_h - T_c) \quad (10)$$

$$H = C\frac{dP}{dT}\lambda + \frac{k_m}{\delta} \quad (11)$$

$$\tau_m = 1/(1 + \frac{H}{h}) \quad (12)$$

$$C = \left[1.064\,\frac{r\varepsilon}{\tau\delta}\left(\frac{M}{RT_m}\right)^{.5} + 0.125\,\frac{r^2\varepsilon}{\tau\delta}\frac{MP_m}{\mathfrak{y}RT_m}\right] \quad (13)$$

Salt mass balance:

$$\frac{d(Vc)}{dt} = -J_s A_m \quad (14)$$

$$V\frac{dc}{dt} + c\frac{dV}{dt} = -J_s A_m \quad (15)$$

$$\frac{dc}{dt} = -\frac{1}{V}\left[J_s A_m + c\frac{dV}{dt}\right] \quad (16)$$

Some notes from the model include:

a- The state variables are: *V, P*
b- The input variables are: q_{in}, T_h, P_o
c- The design variables (parameters) are: *pore size* and *membrane thickness*.
d- The lumped parameter developed model is a function of a single independent variable, *t*.
e- The model parameters are: *C, mass transfer coefficient, h,* k_m, k_s

The governing equations from (3-16) were solved, using the software MATLAB Simulink (The Mathworks, Release 2014b), to determine the change of system permeation with time. The permeate was calculated as the average of accumulated permeate all over the process time.

3.3 Model Verification

To verify the mathematical model, two sets of experiments using fresh water were carried out at temperature ranging from 25°C to 95°C, and different absolute vacuum pressures (800, 600, 400 and 200 mbar), at a fixed feed flow rate of 0.000014 m^3s^{-1} during process time, to study their effects on membrane permeability. Furthermore, experiments performed by different saline solutions (20000, 35000 and 40000 ppm) were also tested to verify the developed model of MD at same conditions previously mentioned. The model was solved firstly considering only Knudsen diffusion, then Knudsen and Poisseuille diffusion (K-P diffusion model) is estimated as total diffusion, and compared with that derived from experimental results. The heat and mass transfer coefficients have been determined for each mentioned system; the temperature polarization coefficient was also calculated.

4 Results and Discussion

4.1 Membrane Performance Evaluation

The performance of the prepared membrane (flux and rejection) was investigated experimentally on the lab-scale unit, using three operating parameters, namely; high concentrated salt solutions, feed temperature and operating vacuum pressure, at a constant feed flow rate (0.000014 m3s-1) and process time (1h).

4.1.1 Effect of Feed Solution Concentrations

Figure 5 (a,b) illustrates the effect of the feed concentration on both permeate flux and salt rejection respectively. As observed from Figure (5a), there is a remarkable decrease in the permeate flux (18.7% decline) from 21.9 to 17.8 Kg m-2h-1 by increasing the feed concentration. According to Raoult's law, the increase in the concentration of the feed decreases the vapor pressure of the feed water, consequently decreases the vapor pressure difference.

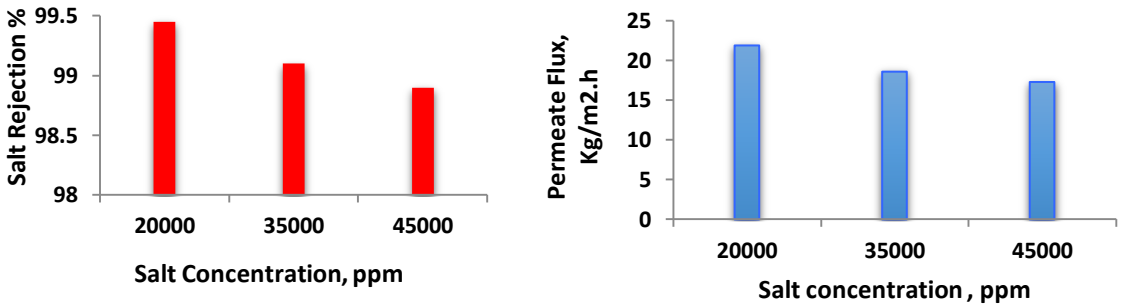

(a) **(b)**

Fig.5: Effect of salt concentration on permeate flux and salt rejection, at feed temperature 65°C, absolute pressure 200 mbar, feed flow rate 0.000014 m^3s^{-1} and 1h process time.

Figure (5b) indicates that the increase in salt concentration leads to a decrease in salt rejection%. This phenomenon is attributed to the fact that the increase in salt concentration at the membrane surface will result in decreasing the mass transfer coefficient of the boundary layer at the feed side due to increasing the influence of concentration polarization [15].

4.1.2 Effect of Feed Temperature

Figures (6-8) demonstrate the experimental results of the permeate flux and corresponding salt rejection, as a function of process time, at different values of both feed temperatures (25-95ºC) and concentrations (20000-40000 ppm).

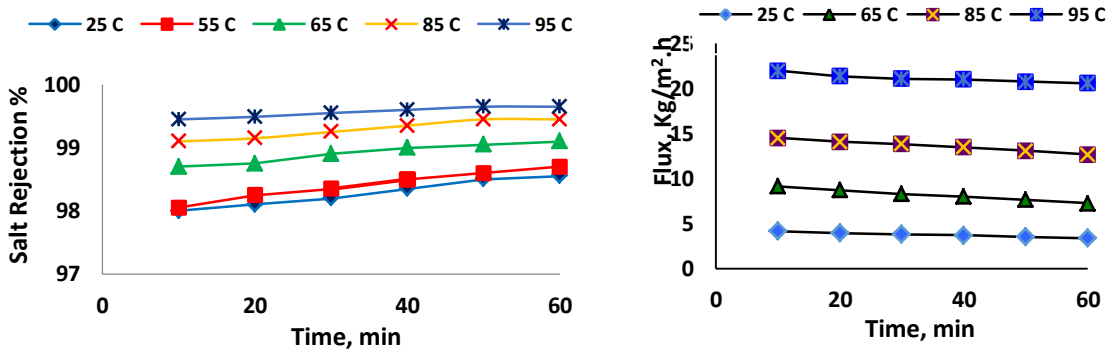

Fig.6: Effect of feed temperature on permeate flux and salt rejection using 20,000 ppm synthetic solution at 200 mbar absolute pressure and 0.000014 m^3s^{-1} flow rate.

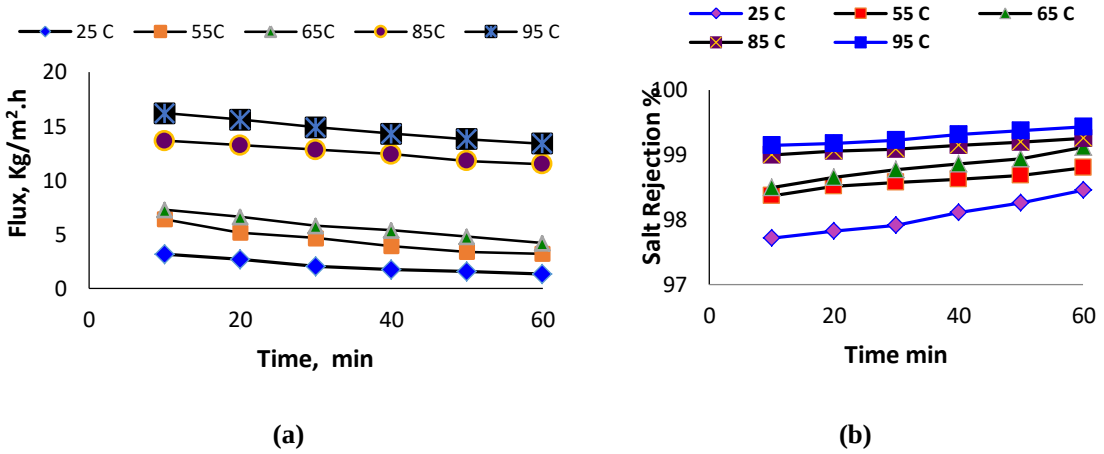

(a) **(b)**

Fig.7: Effect of feed temperature on permeate flux and salt rejection using 35,000 ppm synthetic solution at 200 mbar absolute pressure and 0.000014 m3s-1 flow rate.

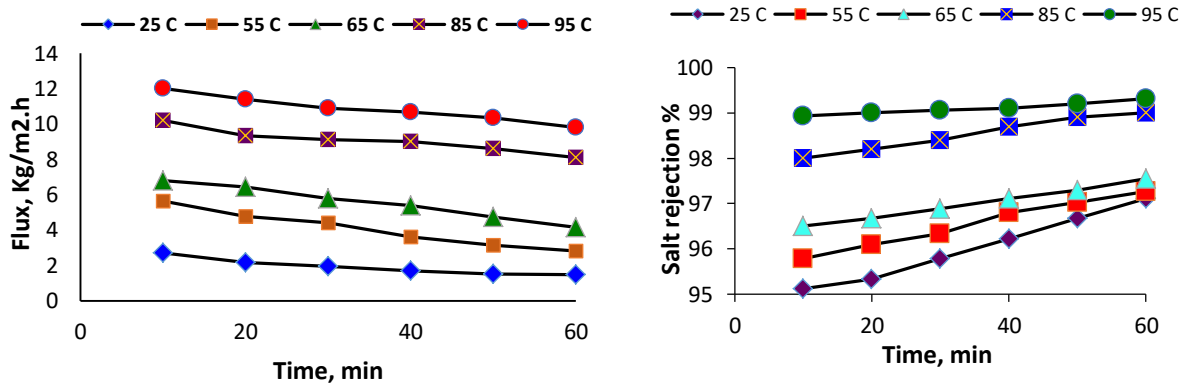

(a) **(b)**

Fig.8: Effect of feed temperature on permeate flux and salt rejection using 40,000 ppm synthetic solution at 200 mbar absolute pressure and 0.000014 m^3s^{-1} flow rate.

They revealed that, for constant feed concentration, the permeate flux has a strong dependence on the feed temperature as shown in Figures (6a-8a). This behavior is expected since, in the VMD process, the main driving force is pressure difference across the membrane. Hence, according to Antoine equation, the vapor pressure of gas-liquid interface on liquid feed side increases with temperature increase, it is positively affecting the diffusion process accompanied by a subsequent increase in the driving force of mass transfer, thus increasing the permeate flux. Figures (6b-8b) illustrate the dependence of salt rejection percent on feed temperature at different solutions concentrations. As observed, the rejection is slightly dependent on temperature. The salt rejection percentage was as high as 99%, 98.7% and 97.2% at 20,000, 35,000, and 40,000 ppm respectively, the gentle decrease is probably due to the concentration polarization effect.

4.1.2 Effect of Operating Pressure at Permeate Side

Figure 9(a,b) illustrates the investigated effect of applied vacuum pressure on membrane performance at different absolute pressures (200-800 mbar). The results, shown in Figure (9a), indicates that the permeate flux increases with decreasing the absolute pressure (increase the vacuum in the system) at permeate side for given operational conditions [15,16]. Generally, in most VMD systems, the transport mechanisms for mass transfer across the membrane are usually based on Knudsen diffusion. Therefore, since the mass flux is depending on the driving force, hence, an increase of vacuum at the downstream of the membrane, at constant feed bulk temperature,

increases the vapor pressure of water and consequently increases the driving force [17,18]. Figure (9b) demonstrates the dependence of salt rejection percent on vacuum pressures. It is evident that salt rejection increased by decreasing the absolute pressure in the system.

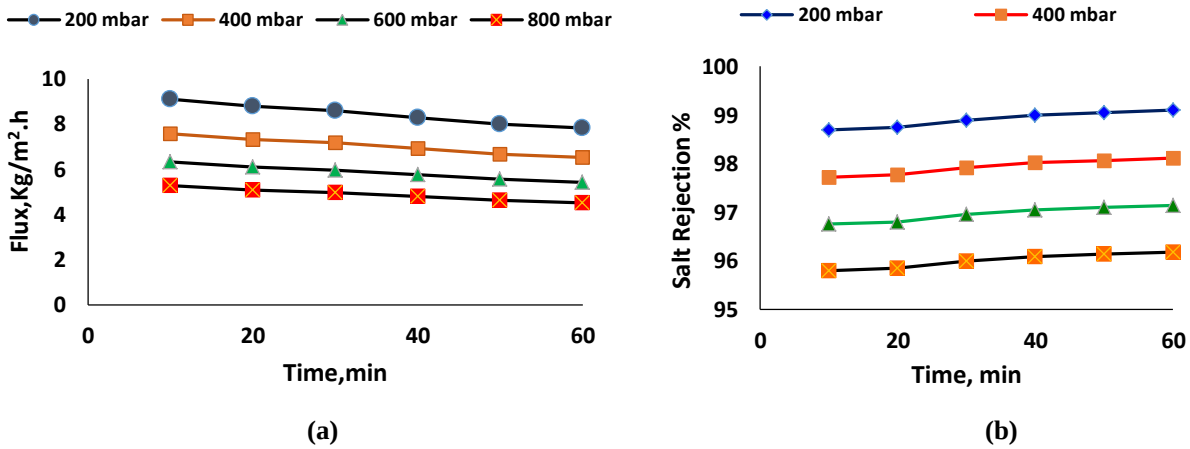

Fig. 9: Effect of vacuum pressure on permeate flux and salt rejection using 20,000 ppm synthetic solution, at 65°C feed temperature and 0.000014 m^3s^{-1} flow rate.

4.2 Model Verification

To investigate the VMD performance, a mathematical model (equations 3-16) is developed and solved using the software MATLAB Simulink (The Mathworks, Release 2014b). The results obtained by the model were in fair agreement with the experimental results, at the same conditions for different feed temperatures considering the Knudsen diffusion model.

Figure (10a) demonstrates the noticeable decrease of the feed tank content with time, this decrease is corresponding to the accumulated permeate volume (product), which is increased with time, as observed in Figure (10b).

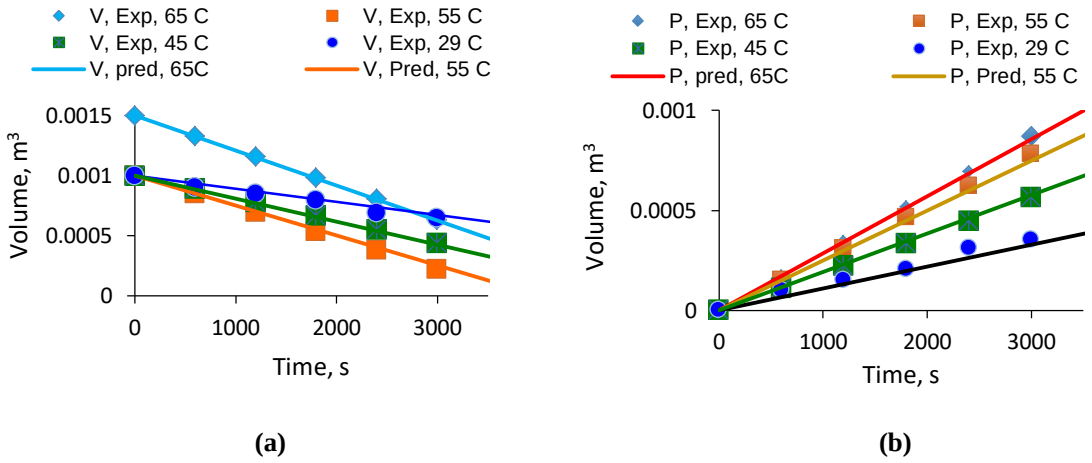

Fig.10: Change of Tank volume (a) and accumulated permeate (b) at different feed temperature.

Table (3) depicts the changes of all variables and parameters (T_h, K, T_c, K, ΔT, T_m, K, P, Pa, C (kn), h, H (kn), τ_m) of the system at different feed temperatures, where $\tau_m = 1/(1 + H/h)$ is the "temperature polarization coefficient", demonstrating the fraction of the total thermal driving force ($T_h - T_c$). Preferably, τ_m should be as close to unity as possible; however, as shown in Table (3), many conditions have τ_m values nearer to zero. It should be noted that τ_m changes with T_m, like H, varies with T_m.

Table 3: Variables and parameters changes in VMD system at different temperature (Knudsen diffusion consideration).

T_h, K	T_c, K	ΔT	T_m, K	P, Pa	C (kn)	h	H (kn)	τ_m, (Kn)
302	298	4	300	3552	0.0904	4100	5.64E+06	0.726
318	309	9	313.5	7575	0.0884	3200	5.11E+06	0.625
328	311	17	319.5	10356	0.0876	2200	5.19E+06	0.424
338	313	25	325.5	13969	0.0868	1750	5.37E+06	0.326

Figure (11) shows the effect of change of flux with changing feed temperature (hot side); it is noticeable that the flux increases with increasing the feed temperature due to the increase in driving force (vapor pressure difference). Also, there is a fair agreement with the experimental results of flux with that predicted using the developed model.

In the temperature range of T_h; from 302 to 338 ºK, the temperature polarization coefficient, τ_m is significantly decreased as the feed temperature increases (Figure 12). This behavior is attributed to the rise of the driving force (vapor pressure gradient) which makes the permeate flux increases substantially (72 $kg.m^{-2}h^{-1}$) with the temperature rise. These larger mass fluxes are accompanied by increasing the heat transfer due to the temperature gradient in the boundary liquid layer; it enhances the phase change, and consequently increase the temperature polarization [14].

The adoption of the integrated K-P diffusion postulated model revealed minor changes in temperature polarization coefficient: a slight decrease occurs as noticed in Figure (12).

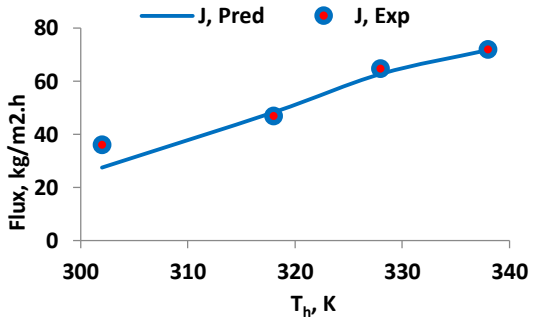

Fig.11: Change of flux with feed temperature.

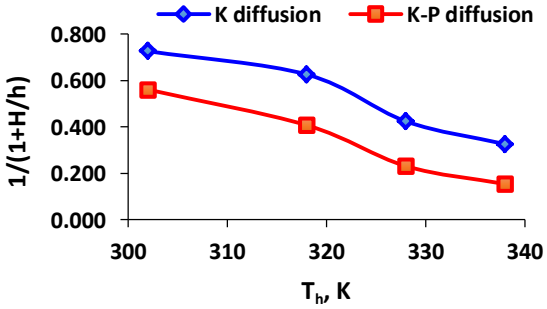

Fig.12: Effect of feed temperature on temperature polarization coefficient considering Knudsen and Knudsen-Poiseuille diffusion.

The feed water concentration is also investigated using a synthetic saline solution of 3440 ppm NaCl concentration, at the same conditions and considering the K-P diffusion model. Figure (13) points that the increase of the accumulated permeate and the feed tank depletion manifest excellent conformity between experimental and predicted model results. Also, the salt concentration in the feed tank increased due to the rejected salts accumulation, Figure (14).

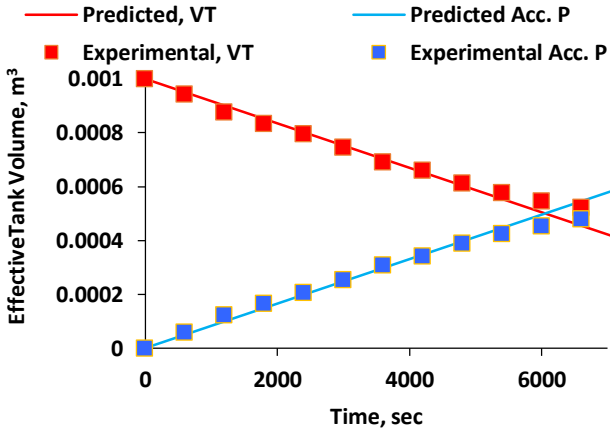

Fig.13: Changes of accumulated permeate and volume depletion with time.

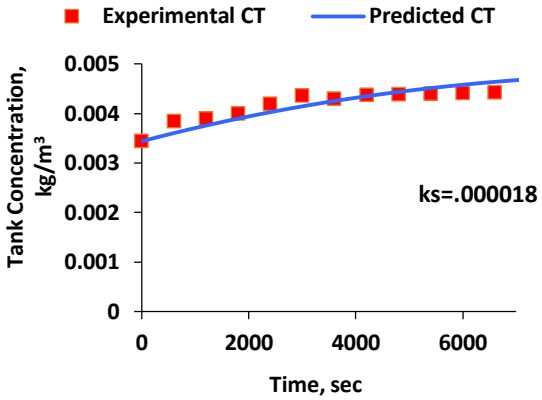

Fig.14: Change of accumulated concentration in feed tank.

4.3 Testing and Evaluation of Pilot VMD Unit Using High Concentrated Salt Solution.

Three different concentrations, namely 25,000, 35,000 and 40,000 ppm, were used to investigate the performance of the designed pilot unit, using the earlier prepared hydrophobic PES/TEOS membrane of permeate flux ranging from 20-30 L/m^{2}h.

4.3.1 Time Dependence on System Performance.

Figures [15(a,b)] illustrate the effect of time on permeate flux and salt rejection respectively at variables feed concentration solutions, ranging between 20000ppm and 40000ppm. The unit operates under constant conditions; temperature (65^{o}C), absolute pressure on the permeate side (300 mbar) and feed flow rate (0.000016 m3s-1).

4.3.2 Dependence of Feed Temperature on System Performance.

The effect of feed temperature on permeate flux has been investigated, from 298 to 338 K, at 0.000016 m^3s^{-1} feed flow rate and 0.03kPa absolute pressure on the permeate side, and time 2 hrs. Figure (16a) illustrates the relationship between the permeate flux and the feed temperature, while Figure (16b) indicates the high salt rejection gained over the feed concentration range studied. As remarked, the same trends were achieved with respect to lab-scale experiments, but with high permeate fluxes.

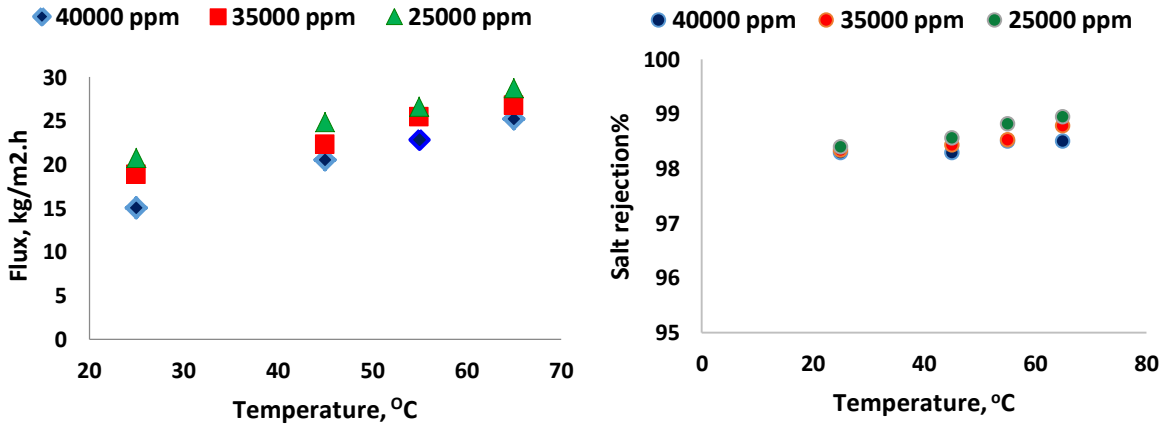

(a) **(b)**

Fig.[16(a,b)]: Effect of feed temperature on permeate flux and salt rejection at different feed concentration solutions.

4.3.3 Dependence of Feed Flow Rate on System Performance.

The effect of feed flow rate, from 0.000008 to 0.000028 m^3s^{-1}, on permeate flux and salt rejection has been investigated as shown in Figures [17(a,b)] respectively, while maintaining all other VMD parameters constant at 338 K (65°C) feed temperature, 0.03 kPa absolute pressure and 2 hrs time.

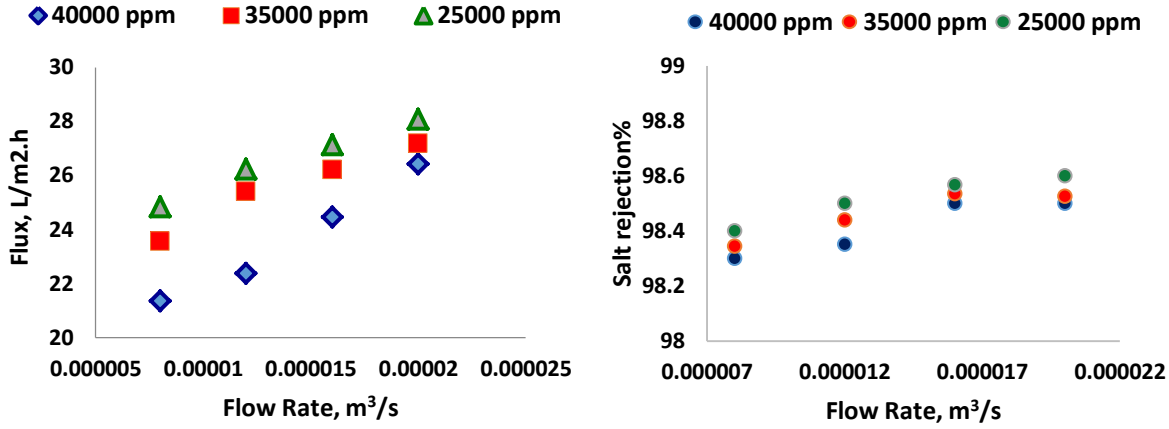

(a) **(b)**

Fig. [17(a,b)]: Effect of feed flow rate on permeate flux and salt rejection at different feed concentration solutions.

As observed in Figure (17a), the flux increases with the rise in feeding rate as well as with reducing the solution concentration. By increasing the volumetric flow rate and consequently the feed velocity, the thermal liquid boundary layer thickness is decreased, resulting in a reduced convective heat and mass transfer resistances, which maximizes the mass transfer coefficient [18- 20]. Figure (17b) demonstrates that the salt rejection percentage increases with increasing feed flow rate and decreases with increasing feed concentrations, due to the increase of concentration polarization.

4.3.4 Effect of backwash on system performance

The backwash method is an efficient physical cleaning method for flux recovery of membranes not rigorously contaminated. The backwash is accomplished by feeding fresh water from down to upper streams of the membrane.

The effect of backwash on system performance (permeate flux and salt rejection) has been investigated at 0.000016 m^3s^{-1} feed flow rate. Experiments were carried out using the prepared hydrophobic PES/TEOS membrane, at 65ºC temperature, 300 mbar vacuum pressure, and 40,000 ppm feed concentration. The backwash occurred after every 5 hrs operating time.

Figures (18,19) demonstrate that both permeate flux and percentage of salt rejection are approximately constant respectively, that may be attributed to the elimination of the direct effect of the concentration polarization by washing, it leads to enhance the permeate flux and salt rejection. Hence, and as expected, the backwash enhances the system performance.

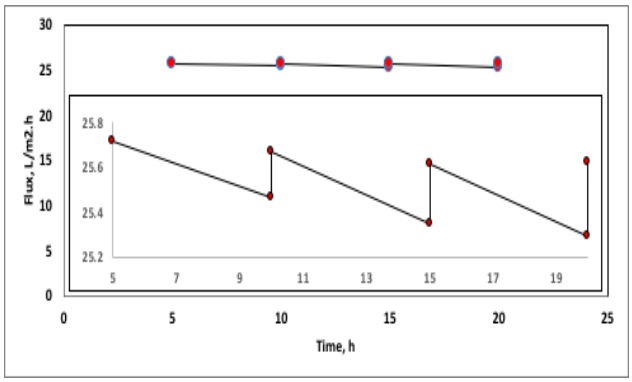

Fig. 18: Effect of backwash on permeate flux.

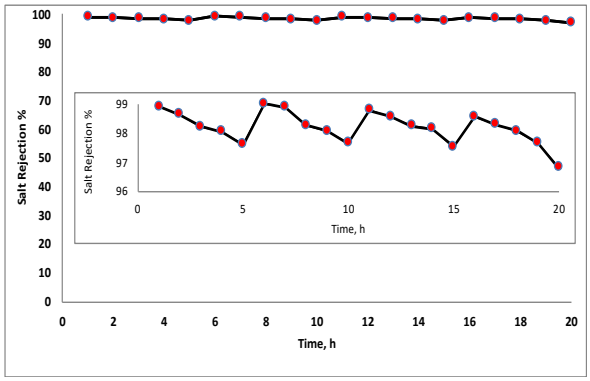

Fig. 19: Effect of backwash on salt rejection.

4.4 Economic Evaluation

4.4.1 Preliminary Economic Evaluation

Assessment of the membrane distillation process, as a new technology for water desalination, a preliminary evaluation is performed based on the information acquired for implementing a pilot unit of 2.6 m^3/day from the local marketing.

4.4.2 Process Design

Based on the results of the performance of the VMD pilot system operating with an average flux of 25 $Lm^{-2}h^{-1}$; the basic design of a scaled-up unit is developed as follows:

1- Design capacity: 2.6 m^3d^{-1}	2- Module: plexy glass plate and frame module of 10 sheets.
3- Area of one membrane sheet: 0.45 m^2	5- Feed temperature: 65^{o}C
4- Total mass transfer area: 4.5 m^2	7- Vacuum pressure: 0.03 kPa
6- Feed flow rate: 0.00003 m^3s^{-1}	9- TDS of product: 200 ppm.
8- TDS of feed water: 40,000 ppm	

Figure (2) illustrates the process-designed flow diagram of the VMD for water desalination, where Figure (20) demonstrates the liquid and vapor paths in10 flat sheets membrane module. Table (4) demonstrates the basic designs of the equipment.

Table 4: Prototype VMD designs characteristics.

Item	Features and operating conditions
Feed Tank	Fiberglass feed tank, volume: 3 m^3, 1.4 m diameter, 2 m height.
Membrane distillation module	Plexy glass holder of polypropylene hydrophobic porous membrane, of square cross section of 0.5*0.5 m^2 (Figure 21).
Brine stream	The brine stream is recycled to the feed tank
Product tank	Fiberglass feed tank, volume: 3 m^3, 1.4m diameter, 2m height.
Heat Exchanger (Condenser)	Stainless steel 316 L condenser with heat transfer area of 0.1 m^2, hot fluid: produced water vapor (T_v = 65°C), cold fluid: feed water (T_f = 25^{o}C)
Feeding Pump	Feed pump: centrifugal pump of stainless steel 316L, with rate of discharge range from 40 cm^3s^{-1} of ¼ Hp. motor drive
Vacuum pump	Double stage vacuum pump, 5×10^{-1}Pa /3.75 Micron, ¾ hp

Figure (2) illustrates the process-designed flow diagram of the VMD for water desalination, where Figure (20) demonstrates the liquid and vapor paths in10 flat sheets membrane module. Table (4) demonstrates the basic designs of the equipment.

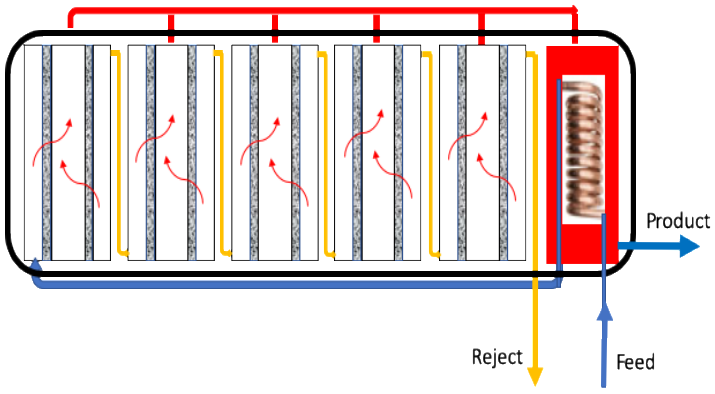

Fig.20: Detailed Design of Membrane Distillation Module.

4.4.3 Product Cost Estimation

Table (5) depicts the price list offered from a local company for purchasing and implementing the prototype unit, based on the above design. This price offer is considered the total direct cost of the unit.

Table 5: Total direct cost of VMD proto-type unit.

Item	Description	Price, LE
1	Membrane holder for 10 membrane sheets, 0.5*0.5 m^2	
2	Unit base	
3	Heater	
4	Temperature degree measuring device	
5	Control panel	
6	Pressure gauge	
7	Steam traps	
Sub total		**260,000**
8	Refrigeration system	12,000
9	Feeding pump, 0.18 kw	18,000
10	Vacuum pump	20,000
11	Two tanks	7000
Total Direct Cost (T.D.C.)		**317,000**

By considering the values of the various percentages of equipment cost, used in evaluating the total direct cost [21], the equipment cost (E) can be estimated by assuming the piping and instrumentation of the unit are equivalent to 30% of the equipment cost. Therefore: *E= TDC/1.3 = 317000/1.3= 243,846 LE.*

Accordingly, the annual operating costs- including the depreciation- are depicted in Table (6).

Table 6: Annual operating costs of VMD proto-type unit.

Item	Price, LE
Depreciation cost (3% of equipment cost, membrane sheets excluded).	7315
Membrane replacement (20% of membrane cost).	8000
Operation & maintenance (2% of equipment cost.)	4877
Energy cost.	2000
Total annual cost.	22,192

The production cost is the sum of the total annual operating cost per unit product capacity. Thus, the unit production cost of desalted water, produced by the VMD system with 90% plant availability, can be calculated as follows:

*Unit Product Cost= 22,192/ 2.6*0.9 *365 = 26 LE (~1.5$).*

This result is in good agreement with early economic analysis, reporting that the unit cost of water produced by a direct contact membrane distillation plant (DCMD) was varying between 1.17$/$m^3$ and 1.23$/$m^3$ with and without heat recovery respectively [22]. Moreover, it is comparable to the cost of water produced by conventional thermal processes, e.g., multiple effect distillation (1.00$/$m^3$) and multi-stage flash distillation (1.40$/$m^3$) [23].

A local offer for reverse osmosis (RO) unit, of 6 m^3/d capacity, was provided from the local market, equivalent to LE500,000. Therefore, reasonable price estimation of a unit of same capacity of the developed MD system; namely, 2.6 m^3/d can be obtained from a scaling factor through the power relationship known as the "six-tenths-factor rule" as expressed in the following equation:

$$\text{Cost of RO unit of } 2.6 m^3 d^{-1} = \text{Cost of RO unit of } 6 m^3 d^{-1} \left[2.6 m^3 d^{-1} / 6 m^3 d^{-1}\right]^{0.6}$$

Hence, the cost of the RO unit delivering 2.6 m^3/d is estimated as LE302, 735.44, by analogy with the VMD previous calculation, the price of production of 1 m^3 by RO is LE17.2 ($0.96). Consequently, it may propose that, further research work concentrating on using low-grade thermal energy resources, for instance, solar energy or surplus heat of a power station, definitely will reduce the cost of water produced by MD to values reaching those of reverse osmosis (RO) technology, which is ranging from 0.48$/$m^3$ to $0.5 /$m^3$, or even less for large-scale units.

5 Conclusions

The performance of a previously prepared PES/TEOS hydrophobic porous membrane was evaluated for water desalination by vacuum membrane distillation system on laboratory and pilot scales. The dependence of different operating factors, namely, feed temperature, downstream vacuum pressure, feed concentration, feed flow rate and process time on the VMD process were thoroughly investigated by monitoring the permeate flux and percent salt rejection. As VMD is a pressure driven process, which varies with temperature, the flux is considerably affected by the feed temperature. The results obtained from the pilot test are in accord with the laboratory experiment results. The designed device exhibited a high degree of desalting at the different operating parameters investigated. The membrane distillation flux reached 25-30 L/m^{2}h (within salinity range studied) at 65°C and 0.03 kPa absolute pressure on the permeate side, while the desalting rate reached 99% on average. Generally, the MD can be used for the treatment of a highly concentrated solution. Furthermore, a mathematical model describing the mechanism and dynamics of the distillation process was developed and verified by experimental results. Thus, it permits under given situations of the vacuum membrane distillation process outlining the ideal characteristics of the membrane desalination process. Assessment of cost indicators revealed that the VMD emerges as being competitive when compared to RO and other thermal desalination technologies when low-cost heat energy is available.

Nomenclature

A_m: Membrane area, m^2
c: concentration, kg.m^{-3}
J: volumetric flux, (m^{3}m^{-2} s^{-1})
h: film heat transfer coefficient, kJ.m^{-2}K^{-1} s^{-1}
k_m: thermal conductivity, kJ.m^{-1}K^{-1} s^{-1}
N: Mass flow rate of water, kg.s^{-1}
P: pressure, Pa
P_o: vacuum pressure at permeate side, Pa
r: membrane pore radius, m
t: time, s
T: temperature, K
C: membrane coefficient, kg.rn^{-2}s^{-1}Pa^{-1}
J_s : salt flux, mol m^{-2}s^{-1}
H: membrane heat transfer coefficient, kJ.m^{-2}K^{-1} s^{-1}
k_s: mass transfer coefficient of salt, m.s^{-1}
M: molecular weight, kgmol^{-1}
N_{Kn}: the mass flux of the Knudsen diffusion, kg.s^{-1}m^{-2}
P_1: vapour pressure of feed water at T_f, Pa
P_m: vapour pressure of water at T_m, Pa
R: universal gas constant, J.mol^{-1} K^{-1}, kg m^2 s $^{-2}$ K $^{-1}$ mol^{-1}
T_m: average temperature at membrane surface, K

Greek symbols

δ: thickness of the membrane, m
λ : heat of vaporization, J.kg^{-1}
P: density, mol.m^{-3}
τ_m: Temperature polarization
ε: membrane porosity
μ: viscosity, Pa. s
τ: *tortuosity*

Subscripts

b: bulk *f : feed* *h: hot* *L: liquid phase* *m: membrane*
p: permeate v: vapor phase

Acknowledgment: Authors would like to show appreciation to Science and Technology Development Fund (STDF), Ministry of Scientific Research Ministry, Egypt, for providing fund to the project entitled "Innovative Technology for Efficient and Cost-Effective Desalination by Membrane Distillation (MD)", Project ID: 552, Project Type: STDF - Water Desalination.

References

[1] A. Alkhudhiri, N. Darwish, N. Hilal, Membrane distillation: A comprehensive review. Desalination., **287**, 2–18, 2012.

[2] M. Gryta, Effectiveness of water desalination by membrane distillation process, Membranes Journal., **2(3)**, 415-429, 2012.

[3] A. Kullab, A. Martin, Membrane distillation and applications for water purification in thermal cogeneration plants, Separation and Purification Technology., **76**, 231–237, 2011.

[4] B. Li, K. K. Sirkar, Novel membrane and device for vacuum membrane distillation-based desalination process, Journal of Membrane Science., **257**, 60–75, 2005.

[5] C. R. Martinetti, A. E. Childress, T. Y. Cath, High recovery of concentrated RO brines using forward osmosis and membrane distillation, Journal of Membrane Science., **331**, 31–39, 2009.

[6] M. A. Izquierdo-Gil, C. Fernández-Pineda, M.G. Lorenz, Flow rate influence on direct contact membrane distillation

experiments: different empirical correlations for Nusselt number, J. Membr. Sci., **321(2)**, 356–363, 2008.

[7] T. D. Dao, J. P. Mericq, S. Laborie, C. Cabassud, A new method for permeability measurement of hydrophobic membranes in Vacuum Membrane Distillation process, Water Research., **47(6)**, 2096- 104, 2013.

[8] E. ElZanati, Innovative Technology for Efficient and Cost-Effective Desalination by Membrane Distillation (MD), project ID 552, funded by Science and Technology Development Fund, Final report., 2015.

[9] E. El-Zanati, M. Khedr, A. El-Gendi, H. Abdallah, E. Farg, E. Taha; Heat and Mass Transfer Characteristics in Vacuum Membrane Distillation for Water Desalination, Deslination and Water Treatment., **134,** 52-62, 2018.

[10] H. Abdallah, A. EL-Gendi, M. Khedr, E. EL-Zanati, Hydrophobic polyethersulfone porous membranes for membrane distillation, Front. Chem. Sci. Eng., **9(1)**, 84–93, 2015.

[11] V. Soni, J. Abildskov, G. Jonsson, R. Gani, Modeling and analysis of vacuum membrane distillation for the recovery of volatile aroma compounds from black currant juice, Journal of Membrane Science., **320**, 442–455, 2008.

[12] O. Makanjuola, I. Janajreh, R. Hashaikeh, Novel technique for fabrication of electrospun membranes with high hydrophobicity retention, Desalination., **436**, 98–106, 2018.

[13] M. A. Salehi, R. Rostamani, Review of membrane distillation for the production of fresh water from saline water, JNAS, **J2-S3**, 1072-1075, 2013.

[14] E. Curcio, E. Drioli, Membrane distillation and related operations a review, Sep. and Purif. Rev., **34**, 35–86, 2005.

[15] F. Kiefer, M. Spinnler, T. Sattelmayer, Multi-Effect Vacuum Membrane Distillation systems: Model derivation and calibration, Desalination., **438**, 97–111, 2018.

[16] M. Khayet, T. Matsuura, Pervaporation and vacuum membrane distillation processes: modeling and experiments, AIChE J., **50(8)**, 1697–1712, 2004.

[17] V. Soni, J. Abildskov, G. Jonsson, R. Gani, Modeling and analysis of vacuum membrane distillation for the recovery of volatile aroma compounds from black currant juice, Journal of Membrane Science., **320**, 442–455, 2008.

[18] T. D. Dao, J. P. Mericq, S. Laborie, C. Cabassud, A new method for permeability measurement of hydrophobic membranes in vacuum membrane distillation process, Water Research., **47(6)**, 2096 – 2104 , 2013.

[19] M. Elma, C. Yacou, J. C. Diniz da Costa and D. K. Wang, Performance and Long-Term Stability of Mesoporous Silica Membranes for Desalination, Membranes., **3(3)**, 136-150, 2013.

[20] S. Srisurichan, R. Jiraratananon, A.G. Fane, Mass transfer mechanisms and transport resistances in direct contact membrane distillation process, J. Membr. Sci., **277 (1)**, 186–194, 2006.

[21] M. S. Peters, and K.D. Trimmerhaus, Plant Design and Economic for Chemical Engineers, McGRAW-HILL, 4th ed. (1991).

[22] S. Al-Obaidani, E. Curcio, F. Macedonio, G. Diprofio, H. Alhinai, E. Drioli, Potential of membrane distillation in seawater desalination: Thermal efficiency, sensitivity study and cost estimation. J. Membr. Sci., **323**, 85–98, 2008.

[23] L. Mar Camacho, L. Dumée, J. Zhang, J. de Li, M. Duke, J. Gomez and S. Gray, Advances in Membrane Distillation for Water Desalination and Purification Applications Water., **5(1)**, 94-196, 2013.